DOI: 10.1002/anie.200604520

Group 5 Azides

Monocapped Trigonal-Prismatic Transition-Metal Heptaazides: Syntheses, Properties, and Structures of $[Nb(N_3)_7]^{2-}$ and $[Ta(N_3)_7]^{2-}$**

Ralf Haiges, Jerry A. Boatz, Muhammed Yousufuddin, and Karl O. Christe**

Dedicated to Professor Neil Bartlett on the occasion of his 75th birthday

During the last decade, inorganic polyazido compounds have received much attention.[1–3] Besides being of academic interest, azides and polyazides are viable candidates for high-energy-density materials (HEDM). The azido group is very energetic, and polyazides are highly endothermic compounds, whose energy content increases with an increasing number of azide ligands. It is, therefore, not surprising that the synthesis of molecules with a high number of azido groups is very challenging owing to their explosive nature and shock sensitivity. Despite such obstacles, a number of pentaazido and anionic hexaazido compounds were reported.[4] Very recently, unprecedented neutral hexaazido species $[M(N_3)_6]$ (M = Mo, W) have been prepared, and, in the case of $[W(N_3)_6]$, also structurally characterized. Treatment of $[M(N_3)_6]$ (M = Mo, W) with ionic azides also yielded the first binary heptaazido compounds.[5] However, due to their high sensitivity, the crystal structures of these heptaazido monoanions could not be determined, and they were solely characterized by low-temperature Raman spectroscopy.

Generally, the stability of a polyazido ion increases with increasing formal negative charge. Therefore, it was felt that the syntheses of heptazido dianions, if possible, might provide a better chance for obtaining structural information. The structures of heptacoordinated species are of particular interest, because the ligands can be arranged in three different ways that differ only very little in energy.[6] They are derived from either a pentagonal bipyramid (1/5/1 arrangement), a monocapped trigonal prism (1/4/2 arrangement), or a monocapped octahedron (1/3/3 arrangement; see Figure 1), and they are readily interconvertible with little or no potential-energy barriers between them.[7]

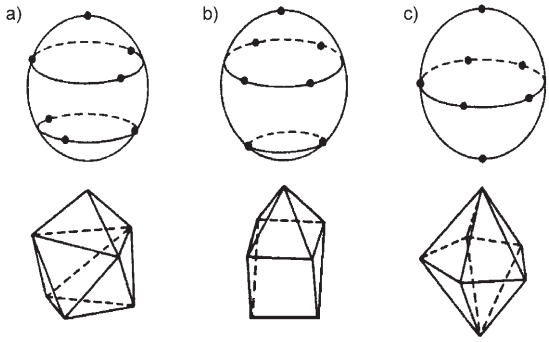

Figure 1. Possible arrangements for heptacoordinated transition metals: a) monocapped octahedron (1/3/3), b) monocapped trigonal prism (1/4/2), and c) pentagonal bipyramid (1/5/1).

Whereas pentagonal-bipyramidal 1/5/1 arrangements are generally observed for the compounds of main-group elements because their bonding involves orthogonal p orbitals of the central atom, for the d-orbital transition metals there appears to be no strong preference for a single structure. For example, $[MoF_7]^-$ and $[WF_7]^-$ exhibit monocapped octahedral structures,[6h] while the solid-state structures of $[TaF_7]^{2-}$ and $[NbF_7]^{2-}$ display monocapped trigonal prisms.[7–9] For the f-orbital actinides, structural preferences become even less pronounced owing to the increased nuclear shielding of the valence electrons. Thus, the $[U(N_3)_7]^{3-}$ trianion was found to crystallize either in the monocapped octahedral 1/3/3 or the pentagonal-bipyramidal 1/5/1 configuration.[10]

It should be noted, however, that heptacoordinated structures exhibit fluxionality and are readily deformed from the idealized 1/3/3, 1/5/1, or 1/4/2 arrangements by the presence of polyatomic ligands, solid-state and packing effects, or the influence of counterions. Therefore, the experimentally observed or the calculated minimum-energy structures are frequently distorted, and the energy differences between calculated minimum-energy structures are not necessarily true measures of the differences between the corresponding idealized structures. Furthermore, the calculated energy differences are sensitive to the level of calculation. In view of these complications, unambiguous experimental data are required to establish the exact structures of these compounds.

[*] Dr. R. Haiges, M. Yousufuddin, Prof. Dr. K. O. Christe
Loker Research Institute and Department of Chemistry
University of Southern California
Los Angeles, CA 90089-1661 (USA)
Fax: (+1) 213-740-6679
E-mail: haiges@usc.edu
kchriste@usc.edu
Dr. J. A. Boatz
Space and Missile Propulsion Division
Air Force Research Laboratory (AFRL/PRSP)
10 East Saturn Boulevard, Bldg 8451
Edwards Air Force Base, CA 93524 (USA)

[**] This work was funded by the Air Force Office of Scientific Research, the Office of Naval Research and the National Science Foundation. We thank Prof. Dr. G. A. Olah for his steady support, and Prof. Dr. R. Bau and Drs. T. Schroer, S. Schneider, W. Wilson, and R. Wagner for their help and stimulating discussions.

Supporting information for this article is available on the WWW under http://www.angewandte.org or from the author.

Herein, we communicate the synthesis and characterization of the first heptaazido dianions, $[Nb(N_3)_7]^{2-}$ and $[Ta(N_3)_7]^{2-}$. In addition, we report the crystal structures of $[P(C_6H_5)_4]_2[Nb(N_3)_7]\cdot CH_3CN$ and $[P(C_6H_5)_4]_2[Ta(N_3)_7]\cdot CH_3CN$, which represent the first structurally characterized transition-metal heptaazides.[11]

While the reactions of $[Nb(N_3)_5]$ and $[Ta(N_3)_5]$ with one equivalent of an ionic azide, such as $[P(C_6H_5)_4]N_3$, yielded the corresponding hexaazido metalates,[4p] it was now found that the reactions with two equivalents of either $[P(C_6H_5)_4]N_3$ in CH_3CN solution or CsN_3 in SO_2 solution can produce salts of the corresponding heptaazido metalate dianions, $[Nb(N_3)_7]^{2-}$ and $[Ta(N_3)_7]^{2-}$, respectively [Eq. (1), M = Nb, Ta; A = $[P(C_6H_5)_4]$, Cs].

$$M(N_3)_5 + 2\,AN_3 \rightarrow A_2[M(N_3)_7] \quad (1)$$

The heptaazido niobates and tantalates were isolated as yellow-orange and pale yellow solids, respectively. The compounds were characterized by the observed material balances, vibrational spectroscopy, and, for the $[P(C_6H_5)_4]^+$ salts, by their crystal structures.[12,13] While the $[P(C_6H_5)_4]^+$ heptaazido monoanion salts of molybdenum and tungsten, $[P(C_6H_5)_4]^+[M(N_3)_7]^-$ (M = Mo, W), are extremely shock-sensitive solids that explode violently when warmed to room temperature and decompose in solution,[5] no such behavior was observed for the dianion salts, $[P(C_6H_5)_4]_2[Nb(N_3)_7]$ and $[P(C_6H_5)_4]_2[Ta(N_3)_7]$, at room temperature. This observation is attributed to the presence of twice as many large counterions, which serve as inert spacers and suppress detonation propagation. For the same reason, the $[P(C_6H_5)_4]_2[M(N_3)_7]$ (M = Nb, Ta) salts are also much less shock-sensitive than neat $[Nb(N_3)_5]$ and $[Ta(N_3)_5]$. Because the Cs^+ cations are less effective spacers than $[P(C_6H_5)_4]^+$, the corresponding $Cs_2[M(N_3)_7]$ salts are also considerably more sensitive than the $[P(C_6H_5)_4]^+$ salts and can explode at room temperature.

Single crystals of $[P(C_6H_5)_4]_2[Nb(N_3)_7]\cdot CH_3CN$ and $[P(C_6H_5)_4]_2[Ta(N_3)_7]\cdot CH_3CN$ were grown by recrystallization from CH_3CN by slowly evaporating the solvent at reduced pressure. The two salts are isostructural and crystallize in the triclinic space group $P\bar{1}$. Their crystal structure analyses[12,13] reveal well-separated $[P(C_6H_5)_4]^+$ and $[M(N_3)_7]^{2-}$ ions and CH_3CN, with no significant cation–anion, anion–anion, or ion–CH_3CN interactions (Figure 2). The closest Nb···N and N···N contacts between neighboring anions are 7.11 Å and 4.02 Å, respectively.[4p]

In these $[P(C_6H_5)_4]_2[M(N_3)_7]\cdot CH_3CN$ salts, the anions (Figure 3) have approximate ideal 1/4/2 arrangements[7] (Table 1). These structures are also similar to one of the two structures previously predicted for $[Mo(N_3)_7]^-$ and $[W(N_3)_7]^-$.[5] The average Nb–N distance (2.13(3) Å) in $[Nb(N_3)_7]^{2-}$ is considerably larger than those found for $[Nb(N_3)_5]\cdot CH_3CN$ and $[Nb(N_3)_6]^-$ (2.00(4) Å and 2.03(3) Å, respectively),[4p] as expected from the higher negative charge in the dianion, which increases the ionic character of the azide ligands. The average Nb-N-N bond angle in $[Nb(N_3)_7]^{2-}$ is 127.5°.

The capped trigonal-prismatic structure of the $[NbF_7]^{2-}$ anion in its dipotassium salt is well-established by both X-ray and neutron diffraction studies.[8,9] Therefore, it was interesting to compare this structure with the experimental and calculated structures of the NbN_7 skeleton of $[Nb(N_3)_7]^{2-}$ and to evaluate the extent of distortions from an ideal 1/4/2 geometry.

On the basis of an ideal 1/4/2 Gillespie–Nyholm VSEPR-type[6,7] model of repelling points on a sphere, all the bond lengths and all the ligand–ligand contacts would be identical, because all ligands are located on the same sphere (Table 1). The upper half of the resulting structure would be a square

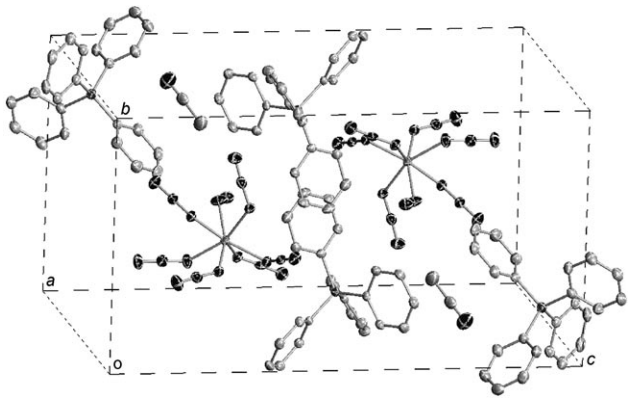

Figure 2. Packing diagram of $[P(C_6H_5)_4]_2[Nb(N_3)_7]\cdot CH_3CN$.

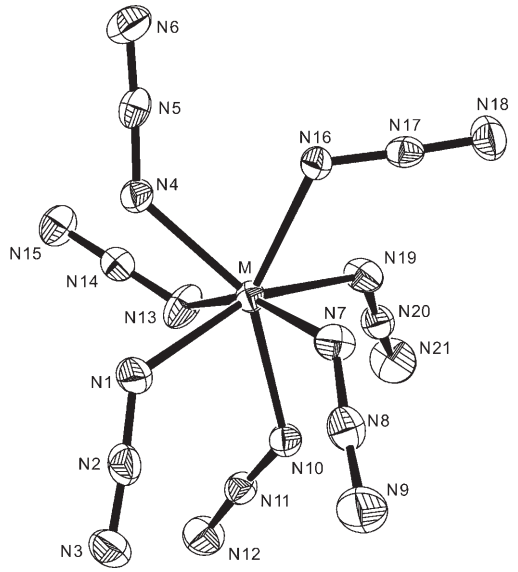

Figure 3. ORTEP drawing of the $[M(N_3)_7]^{-2}$ (M = Nb, Ta) dianions. Thermal ellipsoids are shown at the 50% probability level. Selected bond lengths [Å] and angles [°]: Nb-N1 2.121(2), Nb-N4 2.114(2), Nb-N7 2.091(2), Nb-N10 2.171(2), Nb-N13 2.140(2), Nb-N16 2.140(2), Nb-N19 2.096(2), N1-N2 1.209(3), N2-N3 1.140(3), N7-N8 1.217(3), N8-N9 1.138(3); N1-Nb-N4 74.21(9), N1-Nb-N7 84.0(1), N1-Nb-N10 79.50(9), N1-Nb-N13 90.6(1), N1-Nb-N16 126.23(9), N1-Nb-N19 157.3(1), Nb-N1-N2 130.2(2), N1-N2-N3 176.3(3). Ta-N1 2.096(2), Ta-N4 2.129(2), Ta-N7 2.164(2), Ta-N10 2.130(2), Ta-N13 2.107(2), Ta-N16 2.116(2), Ta-N19 2.087(2), N1-N2 1.210(3), N2-N3 1.139(3), N7-N8 1.202(3), N8-N9 1.146(3); N1-Ta-N4 80.9(1), N1-Ta-N7 78.19(8), N1-Ta-N10 75.13(8), N1-Ta-N13 124.62(8), N1-Ta-N16 156.9(1), N1-Ta-N19 96.1(1), Ta-N1-N2 125.9(2), N1-N2-N3 177.5(3).

Table 1: Comparison of bond lengths [Å] and angles [°] of an ideal capped trigonal prism,[7] the experimental $[NbF_7]^{2-}$ structure,[8,9], and experimental and calculated NbN_7 skeletons in $[Nb(N_3)_7]^{2-}$.

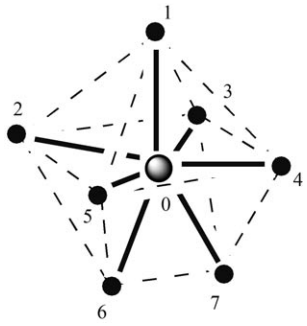

Bond or bond angle	Ideal capped trigonal prism	$[NbF_7]^{2-}$ exptl	NbN_7 exptl	NbN_7 B3LYP	NbN_7 MP2
0-1	all identical	1.96(1)	2.171(2)	2.182	2.148
0-2		1.94(1)	2.091(2)	2.134	2.130
0-3		1.95(1)	2.121(2)	2.184	2.153
0-4		1.96(1)	2.140(2)	2.138	2.134
0-5		1.96(1)	2.096(2)	2.174	2.154
0-6		1.98(1)	2.140(2)	2.174	2.147
0-7		1.96(1)	2.114(2)	2.173	2.146
1-0-2	79.4	79.7(1)	79.6(1)	85.28	86.25
1-0-3	79.4	79.2(1)	79.5(1)	73.98	73.45
1-0-4	79.4	78.7(1)	79.0(1)	87.78	87.40
1-0-5	79.4	76.9(1)	78.3(1)	73.82	73.42
2-0-3	82.6	83.1(1)	84.0(1)	84.38	84.34
2-0-5	97.4	97.7(1)	96.3(1)	99.61	96.55
4-0-5	82.6	80.0(1)	80.9(1)	82.89	83.33
3-0-4	97.4	90.2(1)	90.6(1)	89.22	92.14
6-0-7	73.4	73.9(1)	73.6(1)	72.99	73.29

pyramid with four equilateral triangular faces. The four ligands, 2, 3, 4, and 5, would be perfectly planar. The lower half of the structure would be a trigonal prism, made up of three identical squares, one of them shared with the upper half, and two equilateral triangles identical to those found in the upper half. Because of increased repulsion from the two bottom ligands, 6 and 7, the central four ligands would be located somewhat above the equator of the sphere, and the 2-0-5 and 3-0-4 angles in the central square would be widened to 97.4°, while the corresponding 2-0-3 and 4-0-5 angles would be compressed to 82.6°, but overall C_{2v} symmetry would be retained. As previously shown,[7] the conversion of the capped trigonal prism into the pentagonal bipyramidal 1/5/1 structure results in loss of planarity of the four central ligands, with two opposing ligands above and the other two below the original plane. Therefore, the deviation of the four central ligands from a plane can serve as a measure for the extent to which the 1/4/2 structure is being distorted towards a 1/5/1 structure.

As can be seen in Table 1, the four central ligands in the experimental structures of $[NbF_7]^{2-}$ and the NbN_7 skeleton of $[Nb(N_3)_7]^{2-}$ are almost perfectly planar, and the description of both structures as monocapped trigonal prisms is well-supported by experiment. The excellent agreement between the structures of $[NbF_7]^{2-}$ and the NbN_7 skeleton of $[Nb(N_3)_7]^{2-}$ shows that the azide ligands have little steric impact on the structure of the NbN_7 skeleton and behave as pseudohalogens. However, the calculated B3LYP and MP2 geometries of $[Nb(N_3)_7]^{2-}$ exhibit a pronounced deviation of the four central nitrogen atoms from planarity, indicating that the calculated minimum-energy structures are strongly distorted from the ideal 1/4/2 geometry towards a 1/5/1 arrangement.

The low-temperature Raman spectrum of $Cs_2[Nb(N_3)_7]$ is shown in Figure 4. The Raman spectrum of $Cs_2[Ta(N_3)_7]$ and the observed infrared and Raman spectra of $[P(C_6H_5)_4]_2[Nb(N_3)_7]\cdot CH_3CN$ and $[P(C_6H_5)_4]_2[Ta(N_3)_7]\cdot CH_3CN$ are given as Figures S1–S3 in the Supporting Information. The observed and calculated frequencies and intensities for $[Nb(N_3)_7]^{2-}$ and $[Ta(N_3)_7]^{2-}$ are listed in Tables 2 and 3, respectively. The observed frequencies and intensities are in fair agreement with those calculated, particularly if one considers the difficulties with calculating reliable Raman intensities and the large discrepancies encountered with the use of different computational methods. The vibrations from the azide ligands occur in clusters of seven, one in-phase and six out-of-phase combinations, with the in-phase one being readily identified by its higher Raman intensity. The MN_7 skeletal modes were treated as arising from ideal 1/4/2 structures of C_{2v} symmetry, in accord with our crystal structure and the vibrational analysis of Beuter et al. for heptafluorides.[14] Compared to the neutral pentaazides and hexaazido anions, the addition of a negatively charged N_3^- anion increases the ionicity of the metal–azide bonds and the ionic character of the azide ligands in the $[M(N_3)_7]^{2-}$ anions. With increasing ionic character, the M–N bonds are weakened and both the triple and the single N–N bonds of the covalent azides adopt more double-bond character. This property decreases the stretching frequencies of the N≡N bonds of the N_3 ligands and of the MN_7 skeleton and increases those of the N–N bonds of the N_3 ligands, which is clearly observed in our spectra.

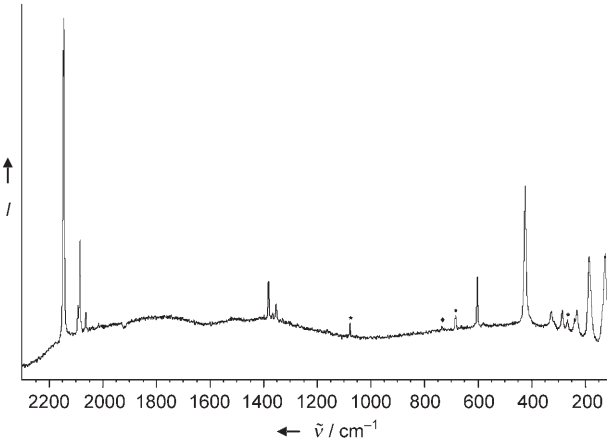

Figure 4. Low-temperature Raman spectrum of solid $Cs_2[Nb(N_3)_7]$. The bands belonging to an impurity of $[SO_2N_3]^-$ are marked by asterisks (*). The band marked with a diamond (◆) is due to the teflon-FEP sample tube; the one marked with a bullet (●) is due to an unidentified impurity.

Table 2: Comparison of observed and unscaled calculated[a] vibrational frequencies [cm^{-1}] and intensities[b] of $Cs_2[Nb(N_3)_7]$.

	Approximate mode description[c]	Observed Raman[d]	Calculated (IR) [Ra] B3LYP		Approximate mode description[c]	Observed Raman[d]	Calculated (IR) [Ra] B3LYP
ν_1		2146 [10.0]	2182 (328) [1042]	ν_{36}		284 [0.6]	278 (64) [3.3]
ν_2		2093 [0.9]	2148 (3032) [63]	ν_{37}			270 (58) [2.4]
ν_3	$\nu_{as}N_3$,	2085 [3.0]	2142 (1516) [117]	ν_{38}	δMN_7,		269 (23) [2.1]
ν_4	one in-phase,		2140 (1773) [143]	ν_{39}	three A_1		260 (13) [3.9]
ν_5	six out-of-phase		2137 (2395) [67]	ν_{40}	two A_2	240 [0.5]	242 (8.1) [5.9]
ν_6		2063 [0.7]	2135 (16) [209]	ν_{41}	three B_1	231 [0.7]	215 (3.4) [5.8]
ν_7		2016 [0.2]	2121 (20) [108]	ν_{42}	three B_2		210 (2.5) [13]
				ν_{43}			203 (0.1) [2.3]
ν_8		1381 [1.2]	1396 (28) [38]	ν_{44}		184 [2.5]	196 (1.4) [8.0]
ν_9			1386 (280) [9.8]	ν_{45}			155 (1.2) [33]
ν_{10}	ν_sN_3,	1366 [0.2]	1382 (79) [22]	ν_{46}		125 [2.5]	137 (5.9) [5.6]
ν_{11}	one in-phase,		1380 (193) [5.8]				
ν_{12}	six out-of-phase	1353 [0.5]	1377 (16) [21]	ν_{47}			135 (5.1) [2.2]
ν_{13}			1375 (291) [4.1]	ν_{48}		101 [4.0]	95 (1.9) [7.2]
ν_{14}		1330 [0.1]	1372 (62) [14]	ν_{49}			89 (0.6) [11]
				ν_{50}			85 (1.7) [14]
ν_{15}			635 (6.8) [1.1]	ν_{51}			82 (2.1) [3.1]
ν_{16}			631 (14) [1.0]	ν_{52}			78 (1.6) [3.8]
ν_{17}	δN_3 in-plane,		629 (11) [0.9]	ν_{53}	torsional		64 (0.2) [15]
ν_{18}	one in-phase,		628 (3.8) [1.0]	ν_{54}	modes		49 (1.1) [14]
ν_{19}	six out-of-phase		625 (3.3) [1.1]	ν_{55}			46 (0.0) [21]
ν_{20}			612 (9.3) [1.5]	ν_{56}			43 (2.9) [4.0]
ν_{21}		602 [1.4]	607 (20) [1.7]	ν_{57}			32 (0.2) [14]
				ν_{58}			31 (0.3) [7.3]
ν_{22}			599 (7.6) [0.7]	ν_{59}			23 (0.3) [6.2]
ν_{23}	δN_3 out-of-plane,		598 (6.6) [1.0]	ν_{60}			17 (0.6) [2.6]
ν_{24}	one in-phase,		591 (6.8) [0.7]				
ν_{25}	six out-of-phase		588 (1.7) [0.5]				
ν_{26}			588 (9.3) [0.2]				
ν_{27}			585 (5.1) [0.2]				
ν_{28}			581 (5.5) [0.4]				
ν_{29}		424 [4.3]	382 (9.6) [93]				
ν_{30}	νMN_7,		377 (353) [4.2]				
ν_{31}	three A_1		371 (305) [7.2]				
ν_{32}	one A_2		366 (292) [0.7]				
ν_{33}	two B_1	325 [0.5]	337 (10) [10]				
ν_{34}	one B_2		329 (21) [14]				
ν_{35}			306 (1.5) [1.9]				

[a] Calculated at the B3LYP/SBKJ + (d) level of theory. [b] Calculated IR intensities are given in parentheses in km mol^{-1}, and Raman intensities in square brackets in $Å^4$ amu^{-1}. [c] The mode assignments for the MN_7 skeletons were made assuming an ideal 1/4/2 arrangement of C_{2v} symmetry. [d] In addition to the bands listed in this table, bands belonging to $SO_2N_3^-$ were observed in the Raman spectrum at 1077 [0.4] and 265 [0.3] cm^{-1}.

In conclusion, $[Nb(N_3)_7]^{2-}$ and $[Ta(N_3)_7]^{2-}$, the first examples of heptaazido dianions, have been prepared. Furthermore, they represent the first structurally characterized transition-metal heptaazides and possess monocapped triangular-prismatic 1/4/2 structures, in accord with those of the corresponding heptafluoride ions in their potassium salts. The structures differ from those found for the actinide heptaazido trianion, $[U(N_3)_7]^{3-}$, which crystallizes either as a monocapped octahedron or a pentagonal bipyramid.

Experimental Section

Caution! Covalent azides are potentially hazardous and can decompose explosively under various conditions! They should be handled only on a scale of less than 1 mmol. Because of the general high energy content and high detonation velocities of most polyazides, their explosions are particularly violent and can cause, even on a 1-mmol scale, significant damage. The use of appropriate safety precautions (safety and face shields, leather gloves, protective clothing, such as heavy leather welding suits, and ear plugs) is mandatory. Teflon containers should be used whenever possible to avoid hazardous shrapnel formation. The manipulation of these materials is facilitated by handling them in solution whenever possible to avoid detonation propagation, by the use of large inert counterions as spacers, and by anion formation, which increases the partial negative charges on the terminal N_γ atoms and thereby reduces the N_β–N_γ triple-bond character. **Ignoring safety precautions can lead to serious injuries!**

Materials and apparatus: All reactions were carried out in teflon-FEP ampules that were closed by stainless steel valves. Volatile materials were handled in a pyrex glass vacuum line. All reaction vessels were passivated with ClF_3 prior to use. Nonvolatile materials were handled in the dry argon atmosphere of a glove box.

Raman spectra were recorded in the teflon reactors at −80 °C in the range 3500–80 cm^{-1} on a Bruker Equinox 55 FT-RA spectrophotometer, using a Nd–YAG laser at 1064 nm with power levels less than

Table 3: Comparison of observed and unscaled calculated[a] vibrational frequencies [cm^{-1}] and intensities[b] of $Cs_2[Ta(N_3)_7]$.

	Approximate mode description[c]	Observed Raman[d]	Calculated (IR) [Ra] B3LYP		Approximate mode description[c]	Observed Raman[d]	Calculated (IR) [Ra] B3LYP
ν_1		2169 [10.0]	2209 (234) [868]	ν_{36}			262 (49) [6.1]
ν_2			2174 (2962) [57]	ν_{37}			260 (49) [3.5]
ν_3	$\nu_{as}N_3$,		2154 (3248) [66]	ν_{38}	δMN_7,		255 (132) [1.7]
ν_4	one in-phase,	2112 [0.8]	2151 (799) [120]	ν_{39}	three A_1	230 [1.8]	253 (94) [6.9]
ν_5	six out-of-phase		2151 (2297) [52]	ν_{40}	two A_2		238 (25) [1.7]
ν_6		2105 [3.2]	2149 (244) [127]	ν_{41}	three B_1		220 (2.5) [4.2]
ν_7		2083 [0.5]	2138 (139) [113]	ν_{42}	three B_2		212 (2.5) [3.7]
				ν_{43}			200 (4.2) [1.4]
ν_8		1408 [0.5]	1432 (17) [95]	ν_{44}		184 [5.0]	195 (4.0) [16]
ν_9			1420 (289) [19]	ν_{45}			163 (0.5) [26]
ν_{10}	ν_sN_3,	1389 [2.8]	1394 (25) [53]	ν_{46}		126 [5.3]	148 (2.9) [1.4]
ν_{11}	one in-phase,		1386 (248) [9.5]				
ν_{12}	six out-of-phase		1386 (277) [7.4]	ν_{47}			144 (4.4) [2.9]
ν_{13}		1376 [0.3]	1385 (37) [21]	ν_{48}		101 [9.0]	94. (1.6) [5.7]
ν_{14}		1363 [1.2]	1384 (85) [20]	ν_{49}			90 (2.5) [4.8]
				ν_{50}			88 (2.4) [9.7]
ν_{15}			629 (6.0) [1.1]	ν_{51}			87 (0.4) [16]
ν_{16}			626 (13) [0.3]	ν_{52}			83 (3.4) [5.2]
ν_{17}	δN_3 in-plane,	630 [0.3]	625 (4.1) [1.0]	ν_{53}	torsional		77 (0. 8) [13]
ν_{18}	one in-phase,		623 (7.6) [0.4]	ν_{54}	modes		51 (4.6) [1.6]
ν_{19}	six out-of-phase		623 (3.5) [1.0]	ν_{55}			44 (2.5) [15]
ν_{20}			609 (11) [0.3]	ν_{56}			39 (0.3) [22]
ν_{21}		603 [2.5]	604 (1.5) [0.2]	ν_{57}			32 (0.7) [9.9]
				ν_{58}			21 (1.5) [2.9]
ν_{22}			602 (16) [0.4]	ν_{59}			20 (0.2) [11]
ν_{23}			601 (2.4) [0.2]	ν_{60}			6 (0.1) [1.3]
ν_{24}	δN_3 out-of-plane,	581 [0.2]	599 (0.6) [0.5]				
ν_{25}	one in-phase,		597 (7.9) [2.5]				
ν_{26}	six out-of-phase		591 (13) [0.4]				
ν_{27}			583 (6.7) [0.3]				
ν_{28}			579 (5.6) [0.6]				
ν_{29}		436 [3.9]	388 (0.1) [77]				
ν_{30}	νMN_7,	388 [0.4]	361 (20) [11]				
ν_{31}	three A_1	345 [0.5]	359 (10) [12]				
ν_{32}	one A_2		346 (161) [1.2]				
ν_{33}	two B_1		343 (169) [0.2]				
ν_{34}	one B_2		335 (283) [2.7]				
ν_{35}			315 (1.8) [1.6]				

[a] Calculated at the B3LYP/SBKJ + (d) level of theory. [b] Calculated IR intensities are given in parentheses in km mol^{-1}, and Raman intensities in square brackets in $Å^4$ amu^{-1}. [c] The mode assignments for the MN_7 skeletons were made assuming an ideal 1/4/2 arrangement of C_{2v} symmetry. [d] In addition to the bands listed in this table, bands belonging to $SO_2N_3^-$ were observed in the Raman spectrum at 2040 [0.8], 2018 [1.2], 1332 [0.2], 1273 [0.5], 1187 [0.3], 1148 [0.0 +], 1077 [3.5], 662 [0.1], 541 [0.3], 426 [1.0], and 266 [3.8] cm^{-1}.

50 mW. Infrared spectra were recorded in the range 4000–400 cm^{-1} on a Midac M Series, FT-IR spectrometer using KBr pellets. The pellets were prepared inside the glove box using an Econo minipress (Barnes Engineering Co.) and transferred in a closed container to the spectrometer before placing them quickly into the sample compartment, which was purged with dry nitrogen.

The starting materials NbF_5, TaF_5 (both Ozark Mahoning) and $[P(C_6H_5)_4]Cl$ (Aldrich) were used without further purification. $(CH_3)_3SiN_3$ (Aldrich) was purified by fractional condensation prior to use. Solvents were dried by standard methods and freshly distilled prior to use. $[Nb(N_3)_5]$ and $[Ta(N_3)_5]$ were freshly prepared from $(CH_3)_3SiN_3$ and NbF_5 or TaF_5 prior to use.[4p] $[P(C_6H_5)_4]N_3$ was obtained from $[P(C_6H_5)_4]Cl$ by anion exchange in aqueous solution.[15] CsN_3 was prepared by a literature method.[16]

Preparation of $[P(C_6H_5)_4]_2[M(N_3)_7]$ salts (M = Nb, Ta): Neat $[P(C_6H_5)_4]N_3$ (0.40 mmol) was added to a frozen solution of $[M(N_3)_5]$ (0.20 mmol) in CH_3CN (25 mmol) at −78 °C. The reaction mixture was warmed to −25 °C and occasionally agitated. After 30 minutes, all volatiles were removed at −20 °C in a dynamic vacuum, leaving behind solid $[P(C_6H_5)_4]_2[M(N_3)_7]$ salts. $[P(C_6H_5)_4]_2[Nb(N_3)_7]\cdot CH_3CN$: orange solid, 0.193 g, expected for 0.20 mmol: 0.221 g. $[P(C_6H_5)_4]_2[Ta(N_3)_7]\cdot CH_3CN$: pale yellow solid, 0.242 g, expected for 0.20 mmol: 0.239 g.

Preparation of $Cs_2[M(N_3)_7]$ salts (M = Nb, Ta): Neat CsN_3 (0.40 mmol) was added to a solution of $[M(N_3)_5]$ (0.20 mmol) in SO_2 (30 mmol) at −78 °C. The reaction mixture was warmed to −45 °C and occasionally agitated. After 30 minutes, a clear yellow solution had formed. The temperature was raised to −40 °C, and all volatiles were removed in a dynamic vacuum, leaving behind 0.20 mmol of the solid $Cs_2[M(N_3)_7]$ salts. An excess of CsN_3 needs to be avoided in these reactions, because it can lead to the formation of some $CsSO_2N_3$ as an impurity. The salts are yellow ($Cs_2[Ta(N_3)_7]$) and orange ($Cs_2[Nb(N_3)_7]$) solids, which are thermally stable at room temperature but can explode on provocation.

Computational methods: The molecular structures and harmonic vibrational frequencies were calculated using previously described methods and basis sets.[5] To check for the different structural isomers, idealized 1/3/3, 1/5/1, or 1/4/2 arrangements were used as starting

points. For $[Nb(N_3)_7]^{2-}$, only one minimum-energy structure was found, independent of the starting point geometry, while for $[Ta(N_3)_7]^{2-}$, two different minimum-energy structures were found. However, these minimum-energy structures were not ideal 1/5/1 and 1/4/2 structures but were significantly distorted. Therefore, the energy differences calculated for the two minimum-energy structures of $[Ta(N_3)_7]^{2-}$ should not be construed as those of ideal 1/5/1 and 1/4/2 geometries. Furthermore, the calculated energy differences were method-dependent. For example, at the MP2 level, the structure obtained from a 1/5/1 starting geometry was favored by 2.9 kcal mol^{-1} over that derived from a 1/4/2 geometry, while at the B3LYP level, the structure obtained with the 1/4/2 starting geometry was preferred by 1.0 kcal mol^{-1}.

Received: November 4, 2006
Published online: March 9, 2007

Keywords: azides · niobium · tantalum · vibrational spectroscopy · X-ray diffraction

[1] A. Kornath, *Angew. Chem.* **2001**, *113*, 3231; *Angew. Chem. Int. Ed.* **2001**, *40*, 3135, and references therein.
[2] C. Knapp, J. Passmore, *Angew. Chem.* **2004**, *116*, 4938; *Angew. Chem. Int. Ed.* **2004**, *43*, 4834.
[3] I. C. Tornieporth-Oetting, T. M. Klapoetke, *Angew. Chem.* **1995**, *107*, 559; *Angew. Chem. Int. Ed. Engl.* **1995**, *34*, 511, and references therein.
[4] a) A. C. Filippou, P. Portius, D. U. Neumann, K.-D. Wehstedt, *Angew. Chem.* **2000**, *112*, 4524; *Angew. Chem. Int. Ed.* **2000**, *39*, 4333; b) A. C. Filippou, P. Portius, G. Schnakenburg, *J. Am. Chem. Soc.* **2002**, *124*, 12396; c) P. Volgnandt, A. Schmidt, *Z. Anorg. Allg. Chem.* **1976**, *425*, 189; d) H. W. Roesky, *Angew. Chem.* **1967**, *79*, 651; *Angew. Chem. Int. Ed. Engl.* **1967**, *6*, 637; e) B. Neumüller, F. Schmock, S. Schlecht, K. Dehnicke, *Z. Anorg. Allg. Chem.* **2000**, *626*, 1792; f) T. M. Klapötke, H. Noeth, T. Schuett, M. Warchhold, *Angew. Chem.* **2000**, *112*, 2197; *Angew. Chem. Int. Ed.* **2000**, *39*, 2108; g) R. Haiges, J. A. Boatz, A. Vij, V. Vij, M. Gerken, S. Schneider, T. Schroer, M. Yousufuddin, K. O. Christe, *Angew. Chem.* **2004**, *116*, 6844; *Angew. Chem. Int. Ed.* **2004**, *43*, 6676; h) K. Karaghiosoff, T. M. Klapoetke, B. Krumm, H. Noeth, *Inorg. Chem.* **2002**, *41*, 170; i) R. Haiges, S. Schneider, T. Schroer, K. O. Christe, *Angew. Chem.* **2004**, *116*, 5027; *Angew. Chem. Int. Ed.* **2004**, *43*, 4919; j) T. M. Klapötke, B. Krumm, P. Mayer, I. Schwab, *Angew. Chem.* **2003**, *115*, 6024; *Angew. Chem. Int. Ed.* **2003**, *42*, 5843; k) R. Haiges, J. A. Boatz, M. Gerken, S. Schneider, T. Schroer, K. O. Christe, *Angew. Chem.* **2003**, *115*, 6027; *Angew. Chem. Int. Ed.* **2003**, *42*, 5847; l) R. Haiges, J. A. Boatz, S. Schneider, T. Schroer, M. Yousufuddin, K. O. Christe, *Angew. Chem.* **2004**, *116*, 3210; *Angew. Chem. Int. Ed.* **2004**, *43*, 3148; m) J. Drummond, J. S. Wood, *Chem. Commun.* **1969**, 1373; n) D. Fenske, H.-D. Doerner, K. Dehnicke, *Z. Naturforsch. B* **1983**, *38*, 1301; o) K. Polborn, E. Leidl, W. Beck, *Z. Naturforsch. B* **1988**, *43*, 1206; p) R. Haiges, J. A. Boatz, T. Schroer, M. Yousufuddin, K. O. Christe, *Angew. Chem.* **2006**, *118*, 4948; *Angew. Chem. Int. Ed.* **2006**, *45*, 4830.
[5] R. Haiges, J. A. Boatz, R. Bau, S. Schneider, T. Schroer, M. Yousufuddin, K. O. Christe, *Angew. Chem.* **2005**, *117*, 1894; *Angew. Chem. Int. Ed.* **2005**, *44*, 1860.
[6] a) R. J. Gillespie, I. Hargittai, *The VSEPR Model of Molecular Geometry*, Allyn and Bacon, A Dvision of Simon Schuster, Needham Heights, MA, **1991**; b) R. Hoffmann, B. F. Beier, E. L. Muetterties, A. R. Rossi, *Inorg. Chem.* **1977**, *16*, 511; c) D. Kepert, *Inorganic Stereochemistry*, Springer, Berlin, **1982**; d) T. A. Claxton, G. C. Benson, *Can. J. Chem.* **1966**, *44*, 157; e) H. Bradford Thompson, L. S. Bartell, *Inorg. Chem.* **1968**, *7*, 488; f) H. K. McDowell, H.-L. Chiu, J. F. Geldard, *Inorg. Chem.* **1988**, *27*, 1674; g) G. W. Drake, D. A. Dixon, J. A. Sheehy, J. A. Boatz, K. O. Christe, *J. Am. Chem. Soc.* **1998**, *120*, 8392, and references therein; h) S. Giese, K. Seppelt, *Angew. Chem.* **1994**, *106*, 473; *Angew. Chem. Int. Ed. Engl.* **1994**, *33*, 461.
[7] M. C. Favas, J. M. Harrowfield, D. L. Kepert, B. W. Skelton, L. M. Vitolo, A. H. White, *Aust. J. Chem.* **1992**, *45*, 1547.
[8] J. L. Hoard, *J. Am. Chem. Soc.* **1939**, *61*, 1252.
[9] G. M. Brown, L. A. Walker, *Acta Crystallogr.* **1966**, *20*, 220.
[10] M.-J. Crawford, A. Ellern, P. Mayer, *Angew. Chem.* **2005**, *117*, 8086; *Angew. Chem. Int. Ed.* **2005**, *44*, 7874.
[11] Preliminary results from this study were previously reported at the Molecular Dynamics Conference in Monterey, CA, on May 23, 2005, the 3rd Energetic Materials Technology Exchange in Arlington, VA on July 12, 2005, and the 17th International Symposium on Fluorine Chemistry in Shanghai, China on July 29, 2005.
[12] Crystal data for $C_{50}H_{43}N_{22}NbP_2$: $M_r = 1106.91$, triclinic, space group $P\bar{1}$, $a = 10.767(1)$, $b = 11.229(1)$, $c = 24.053(2)$ Å, $\alpha = 83.196(2)$, $\beta = 81.576(2)$, $\gamma = 61.545(1)°$, $V = 2525.2(4)$ Å^3, $F(000) = 1136$, $\rho_{calcd} = 1.456$ g cm^{-3}, $Z = 2$, $\mu = 0.363$ mm^{-1}, crystal size $0.32 \times 0.25 \times 0.09$ mm^3, θ range 1.71 to 27.45°, index ranges $-13 \le h \le 13$, $-14 \le k \le 10$, $-25 \le l \le 31$, $Mo_{K\alpha}$ ($\lambda = 0.71073$ Å), $T = 133(2)$ K, 15500 measured data (Bruker 3-circle, SMART APEX CCD with χ axis fixed at 54.74°, using the SMART V 5.625 program, Bruker AXS: Madison, WI, 2001), of which 10839 ($R_{int} = 0.0275$) unique. Lorentz and polarization correction (SAINT V 6.22 program, Bruker AXS: Madison, WI, 2001), absorption correction (SADABS program, Bruker AXS: Madison, WI, 2001), transmission factors min/max ratio 0.803. Structure solution by direct methods (SHELXTL 5.10, Bruker AXS: Madison, WI, 2000), full-matrix least-squares refinement on F^2, data/parameters ratio 16.0:1, final R indices [$I > 2\sigma(I)$]: $R1 = 0.0436$, $wR2 = 0.0976$, R indices (all data): $R1 = 0.0647$, $wR2 = 0.1039$, GOF on $F^2 = 1.024$. CCDC-269626 contains the supplementary crystallographic data for this paper. These data can be obtained free of charge from the Cambridge Crystallographic Data Centre via http://www.ccdc.cam.ac.uk/data_request/cif.
[13] Crystal data for $C_{50}H_{43}N_{22}P_2Ta$: $M_r = 1194.95$, triclinic, space group $P\bar{1}$, $a = 10.7596(9)$, $b = 11.243(1)$, $c = 24.043(2)$ Å, $\alpha = 83.158(1)$, $\beta = 81.591(1)$, $\gamma = 61.617(1)°$, $V = 2527.3(4)$ Å^3, $F(000) = 1200$, $\rho_{calcd} = 1.570$ g cm^{-3}, $Z = 2$, $\mu = 2.299$ mm^{-1}, crystal size $0.37 \times 0.36 \times 0.15$ mm^3, θ range 1.72 to 27.54°, index ranges $-10 \le h \le 13$, $-10 \le k \le 14$, $-31 \le l \le 31$, $Mo_{K\alpha}$ ($\lambda = 0.71073$ Å), $T = 123(2)$ K, 15609 measured data (Bruker 3-circle, SMART APEX CCD with χ axis fixed at 54.74°, using the SMART V 5.625 program, Bruker AXS: Madison, WI, **2001**), of which 10936 ($R_{int} = 0.0207$) unique. Lorentz and polarization correction (SAINT V 6.22 program, Bruker AXS: Madison, WI, **2001**), absorption correction (SADABS program, Bruker AXS: Madison, WI, **2001**), transmission factors min/max ratio: 0.785. Structure solution by direct methods (SHELXTL 5.10, Bruker AXS: Madison, WI, **2000**), full-matrix least-squares refinement on F^2, data/parameters ratio 16.0:1, final R indices [$I > 2\sigma(I)$]: $R1 = 0.0242$, $wR2 = 0.0635$, R indices (all data): $R1 = 0.0258$, $wR2 = 0.0641$, GOF on $F^2 = 1.041$. CCDC-269627 contains the supplementary crystallographic data for this paper. These data can be obtained free of charge from the Cambridge Crystallographic Data Centre via http://www.ccdc.cam.ac.uk/data_request/cif.
[14] A. Beuter, W. Kuhlmann, W. Sawodny, *J. Fluorine Chem.* **1975**, *6*, 367.
[15] R. Haiges, T. Schroer, M. Yousufuddin, K. O. Christe, *Z. Anorg. Allg. Chem.* **2005**, *631*, 2691.
[16] M. Gerken, S. Schneider, T. Schroer, R. Haiges, K. O. Christe, *Z. Anorg. Allg. Chem.* **2002**, *628*, 909.

